

# Role of structural flexibility in the fluorescence and photochromism of salicylideneaniline: the general scheme of the phototransformations

M.E. Kletskii, A.A. Millov, A.V. Metelitsa, M.I. Knyazhansky\*

*Institute of Physical and Organic Chemistry, Rostov State University, Stachki Str. 194/2, Rostov on Don 344090, Russia*

Received 9 June 1997; accepted 12 June 1997

## Abstract

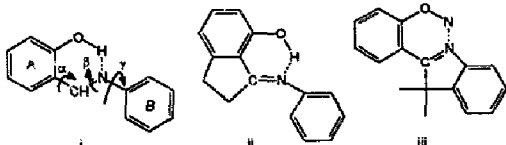
The mechanism of light-induced transformation in the salicylideneaniline molecule was studied by semiempirical PM3 calculations. The structures and energies of the minima and saddle points (transition states) on the  $S_0$ ,  $S_1$  and  $T_1$  potential energy hypersurfaces (PESs) were obtained, together with the gradient lines on the PESs. The structure–energy scheme was compared with the experimental findings. According to the results obtained, the following principle processes are observed: fast  $S_1$  excited state intramolecular proton transfer (ESIPT), followed by typical ESIPT fluorescence; the formation of two  $S_1$  twisted intramolecular charge transfer (TICT) structures which quench the ESIPT fluorescence; the diabatic formation of two ground state metastable coloured “post-TICT” structures responsible for photochromism.  
© 1997 Elsevier Science S.A.

**Keywords:** Anomalous Stokes shift; Excited state intramolecular proton transfer (ESIPT); Fluorescence; Photochromism; Photocoloured structures; “Post-TICT” structures; Potential energy surfaces; Salicylideneaniline; Twisted intramolecular charge transfer (TICT)

## 1. Introduction

The salicylideneaniline molecule is a highly useful model compound for the investigation of the role of structural flexibility in light-induced structural transformations. It includes fragments providing an opportunity for excited state intramolecular proton transfer (ESIPT)  $\text{OH} \rightarrow \text{NH}$ , followed by single and double bond twisting, which can be clearly observed as typical fluorescence and photochemical (including photochromic) properties [1–4].

In Ref. [4], comparative experimental investigations and preliminary quantum chemical calculations were carried out for salicylideneaniline (i) and more rigid model structures (ii and iii) to determine the mechanisms responsible for the fluorescence and photochromic properties of i.



The key role of the “aldehyde” ring (A) twist has been ascertained in the formation of the fluorescence quenching

twisted intramolecular charge transfer (TICT) and photocoloured structures.

However, the molecular structure of the latter was proposed on the basis of data from preliminary spectral quantum chemical CNDO/S calculations. In this work, a detailed quantum chemical investigation of the light-induced processes in molecule i is performed to interpret the experimental findings and to construct a structure–energy scheme, including the mechanisms of formation of the fluorescence, fluorescence quenching and photocoloured structures.

## 2. Method of quantum chemical studies

The geometries of all the compounds under consideration were fully optimized using the semiempirical method PM3 [5], with the mopac program [6]. The restricted Hartree–Fock (RHF) procedure was used for closed-shell species and the half-electron method [7] was used for open-shell species.

The reaction pathways leading to a mechanism of reaction in each electronic state ( $S_0$ ,  $S_1$  and  $T_1$ ) were studied as relevant gradient lines on the potential energy hypersurfaces (PESs) [8]. All critical points on these gradient lines were characterized by the number of Hessian negative eigenvalues (indices  $\lambda$ ) [9]. The experimental methods and findings have been described in detail previously [4].

\* Corresponding author.

### 3. Results and discussion

Fig. 1, Fig. 2 and Table 1 show the data obtained from the quantum chemical studies and the experimental findings.

In accordance with the experimental findings, the calculated data (see Table 1) indicate that the initial enol form ( $E^{S_0}$ ) in the trans (about the C=N bond) structure ( $\beta=0$ ) with the flat aldehyde fragment ( $\alpha=0$ ) is stabilized by a strong intramolecular H bond (O-H...N) [4]. The following steps in the overall light-induced process are realized.

(I) The excited  $E^{S_1}$  structure is formed on excitation ( $S_0 \rightarrow S_1$ ) of the initial  $E^{S_0}$  structure. The former is characterized by charge transfer from the OH group to the C=N group ( $\Delta q \sim 0.35 e$ ).

(II) Such an alteration in the acidity and basicity of the OH and C=N groups respectively in the  $S_1$  state promotes a low-energy barrier ( $\Delta E \sim 1.7 \text{ kJ mol}^{-1}$ ) (or tunnelling) fast ESIPT, leading to the formation of the planar polar ( $\mu_K^{S_1} = 9.74 \text{ D}$ ) "keto" structure  $K^{S_1}$  (Table 1) situated on the clearly expressed inclined energetic plateau. This structure is

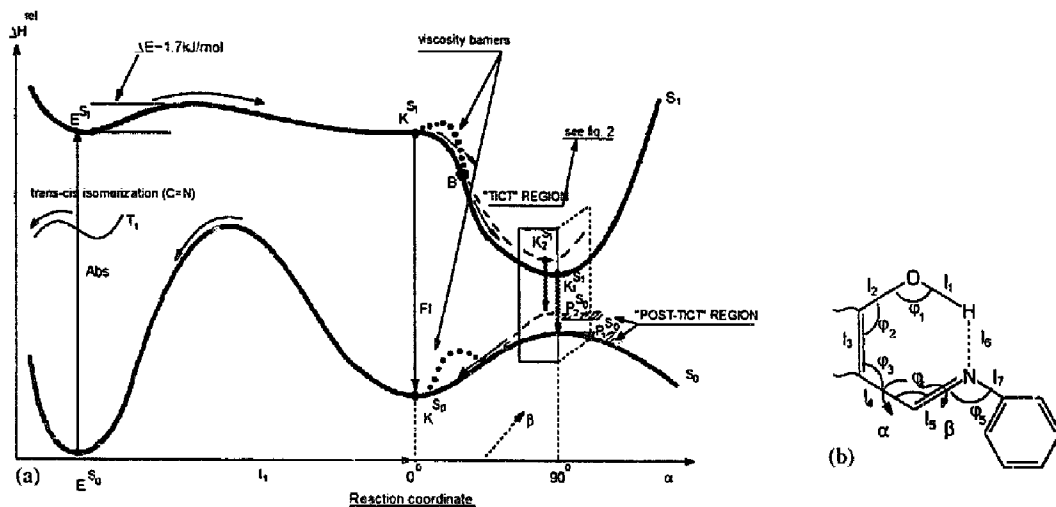


Fig. 1. Schematic representation of the  $S_0$  and  $S_1$  PES sections (PM3 calculations) along the minimum energy paths (a) and the main geometrical parameters of the reactions considered here (b).

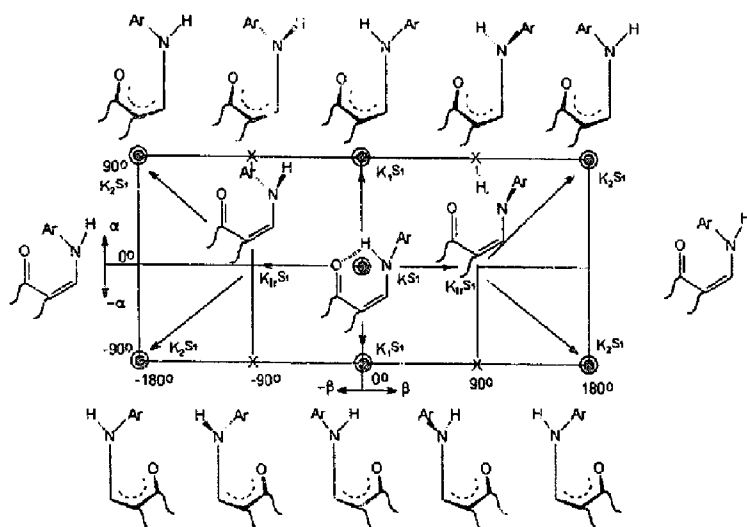


Fig. 2. Detailed representation of the region between  $K^{S_1}$  and "TICT" structures on the  $S_1$  PES (see Fig. 1). Reaction paths are marked with double circles.

Table 1  
Main geometrical data, heats of formation ( $\Delta H_f$ ) and dipole moments ( $\mu$ ) calculated for the different structures cited in the text (for notation, see Fig. 1)

| Parameter                            | E <sup>S<sub>0</sub></sup> | E <sup>S<sub>1</sub></sup> | K <sup>S<sub>0</sub></sup> | K <sup>S<sub>1</sub></sup> | K <sub>1</sub> <sup>S<sub>1</sub></sup> | K <sub>2</sub> <sup>S<sub>1</sub></sup> | K <sub>3</sub> <sup>S<sub>1</sub></sup> | P <sub>1</sub> <sup>S<sub>0</sub></sup> | P <sub>2</sub> <sup>S<sub>0</sub></sup> |
|--------------------------------------|----------------------------|----------------------------|----------------------------|----------------------------|---|---|---|---|---|
| $\Delta H_f$ (kJ mol <sup>-1</sup> ) | 90.8                       | 461.5                      | 126.8                      | 397.9                      | 319.2                                   | 333.0                                   | 366.9                                   | 246.0                                   | 269.0                                   |
| $\mu$ (D)                            | 2.5                        | 1.3                        | 3.3                        | 9.7                        | 14.4                                    | 13.3                                    | 7.3                                     | 3.5                                     | 3.8                                     |
| Bond lengths (nm)                    |                            |                            |                            |                            |   |   |   |   |   |
| $l_1$                                | 0.097                      | 0.098                      | 0.183                      | 0.178                      | 0.326                                   | 0.407                                   | 0.276                                   | 0.316                                   | 0.300                                   |
| $l_2$                                | 0.135                      | 0.133                      | 0.124                      | 0.127                      | 0.125                                   | 0.125                                   | 0.125                                   | 0.123                                   | 0.123                                   |
| $l_3$                                | 0.141                      | 0.146                      | 0.147                      | 0.146                      | 0.144                                   | 0.144                                   | 0.146                                   | 0.147                                   | 0.148                                   |
| $l_4$                                | 0.146                      | 0.142                      | 0.139                      | 0.148                      | 0.144                                   | 0.144                                   | 0.140                                   | 0.141                                   | 0.141                                   |
| $l_5$                                | 0.130                      | 0.135                      | 0.137                      | 0.134                      | 0.132                                   | 0.132                                   | 0.140                                   | 0.138                                   | 0.138                                   |
| $l_6$                                | 0.183                      | 0.173                      | 0.102                      | 0.102                      | 0.100                                   | 0.100                                   | 0.100                                   | 0.100                                   | 0.100                                   |
| $l_7$                                | 0.143                      | 0.141                      | 0.144                      | 0.143                      | 0.146                                   | 0.145                                   | 0.138                                   | 0.143                                   | 0.143                                   |
| Valence angles (°)                   |                            |                            |                            |                            |   |   |   |   |   |
| $\phi_1$                             | 108                        | 109                        | 106                        | 107                        | 72                                      | 85                                      | 102                                     | 83                                      | 88                                      |
| $\phi_2$                             | 124                        | 124                        | 121                        | 121                        | 122                                     | 122                                     | 120                                     | 122                                     | 122                                     |
| $\phi_3$                             | 123                        | 122                        | 122                        | 120                        | 118                                     | 118                                     | 120                                     | 120                                     | 120                                     |
| $\phi_4$                             | 119                        | 117                        | 121                        | 120                        | 117                                     | 125                                     | 122                                     | 122                                     | 128                                     |
| $\phi_5$                             | 123                        | 124                        | 122                        | 124                        | 123                                     | 131                                     | 125                                     | 120                                     | 128                                     |
| Dihedral angles (°)                  |                            |                            |                            |                            |   |   |   |   |   |
| $\alpha$                             | 0                          | 0                          | 0                          | 0                          | 90                                      | 90                                      | 0                                       | 90                                      | 90                                      |
| $\beta$                              | 0                          | 0                          | 0                          | 0                          | 0                                       | 180                                     | 90                                      | 0                                       | 180                                     |

responsible for the fluorescence ( $\varphi_f \sim 0.001$ ) with an anomalous Stokes shift (ASS fluorescence) arising only in rigid media at low temperature ( $T \sim 77$  K) [4]. Similar fluorescence ( $\varphi_f \sim 0.044$ ) is typical of the model rigid structures ii and iii in both rigid and liquid solutions at room temperature [4]. This testifies to the significant role of the "viscosity" barrier localized on the energetic plateau. The barrier inhibits the subsequent ESIPT  $S_1$  state structure changes and is responsible for ASS fluorescence quenching in low-viscosity media.

(III) Such structural changes proceed from the bifurcation point (B) on the energetic plateau along two different pathways on the  $S_1$  state PES:

(a) transformations associated with the variation of the dihedral angle  $\alpha$  only (twist about the C-C bond), resulting in the formation of the high-polar ( $\mu_{K_1^{S_1}} = 14.4$  D) twisted ( $\alpha = 90^\circ$ ) trans (around the C-N bond,  $\beta = 0^\circ$ )  $K_1^{S_1}$  structure (TICT<sub>1</sub> structure) (see Table 1, Fig. 1 and Fig. 2);

(b) more complex conformation changes associated initially with a variation in the  $\beta$  dihedral angle only (i.e. twist around the C-N bond), leading to the transient  $K_{tr}^{S_1}$  structure,  $\beta = 90^\circ$ , followed by concerted variations of both angles ( $\alpha$  and  $\beta$ ), resulting in another high-polar twisted cis (around the C-N bond,  $\alpha = 90^\circ$ ,  $\beta = 180^\circ$ ) structure  $K_2^{S_1}$  (TICT<sub>2</sub> structure) ( $\mu_{K_2^{S_1}} = 13.3$  D) (Table 1 and Fig. 2).

(IV) As a result of the proximity of the  $S_0$  and  $S_1$  state PESs in the neighbourhood of the TICT<sub>1</sub> and TICT<sub>2</sub> structures, the intense radiationless deactivation  $S_1 \rightarrow S_0$  is respon-

sible for the almost complete ASS fluorescence quenching in low-viscosity media [4] (Fig. 1).

(V) Diabatic processes lead to the formation of two different (see Refs. [2,10]) metastable twisted "post-TICT" structures  $P_1^{S_0}$  and  $P_2^{S_0}$  on the  $S_0$  state PES differing slightly from the corresponding TICT<sub>1,2</sub> structures (see Table 1 and Fig. 1). These extremely twisted structures are stabilized by the viscous media and are responsible for the photoinduced colouration ( $\lambda^{abs} = 480$  and 540 nm according to experimental data [4] and 460 and 530 nm respectively in CNDO/S calculations). The equilibrium  $P_1^{S_0} \rightleftharpoons P_2^{S_0}$  can occur as a function of the temperature and solvent polarity. According to this scheme, the photochromism typical of i is not observed for the model structures ii and iii; this is confirmed by experiment [4].

(VI) According to the experimental findings [1,2], the removal of the "viscosity barrier" leads to fast reverse structural changes in the  $S_0$  state associated with the formation of the planar keto structure  $K^{S_0}$  (Table 1 and Fig. 1) and subsequent transformation  $K^{S_0} \rightarrow E^{S_0}$  due to back (NH  $\rightarrow$  OH) ground state intramolecular proton transfer.

(VII) The ground state thermally reversible process of trans-cis photoisomerization mainly occurs in the  $T_1$  state of the E structure by rotation (but not inversion) about the C=N bond with OH...N bond disruption. This is confirmed by the findings obtained on T-T sensitization of this reaction [2].

#### 4. Conclusions

In the scheme described above, the crucial role of the structural flexibility is shown in the photoinduced processes

occurring in the salicylideneaniline molecule (i), in contrast with the less flexible structures ii and iii.

The scheme agrees completely with the experimental findings and provides a more detailed mechanism of the light-induced processes compared with that described previously [4].

The most important peculiarities are the fast adiabatic ESIPT, followed by ASS fluorescence, the formation of two TICT structures and the key role played by the twisted "aldehyde" ring in ASS fluorescence quenching as well as in the diabatic formation of two different (not single!) [2,10] metastable ground state "post-TICT" structures ("keeping in mind" the real TICT structures) which cause the photochromic properties of the salicylideneaniline molecule.

The suggested mechanisms of fluorescence and photochromism on steady state excitation in rigid media are extremely different from those discussed previously [1] and those derived from recent kinetic investigations [3].

Therefore it is important to continue our investigations of i-type molecules with the aim of coordinating the kinetic and structural data to obtain a uniform interpretation of the photoinduced processes in these compounds.

## Acknowledgements

This work was supported by a Grant for Scientific Research (97-03-32017a) from the Russian Fund of Fundamental Investigations (RFFI).

## References

- [1] E. Hadjoudis, in H. Durr, 'I. Bouas-Laurent (Eds.), Photochromism, Molecules and Systems, Elsevier, Amsterdam, 1990, p. 685.
- [2] M.I. Knyazhansky, A.V. Metelitsa, Photoinduced Processes in the Azomethine Molecules and Their Structural Analogs, Rostov University Publishing House, Rostov on Don, 1992, pp. 77–136 (in Russian).
- [3] J.S. Stephan, A. Mordzinski, C. Rios Rodriguez, K.H. Grellman, Chem. Phys. Lett. 229 (1994) 541.
- [4] M.I. Knyazhansky, A.V. Metelitsa, A.Ja. Bushkov, S.M. Aldoshin, J. Photochem. Photobiol. A: Chem. 97 (1996) 121.
- [5] J.J.P. Stewart, J. Comput. Chem. 10 (1989) 209.
- [6] J.J.P. Stewart, mopac 7.0: A Semiempirical Molecular Orbital Program, Program No. 455, Quantum Chemistry Program Exchange (QCPE), Indiana University, Bloomington, IN 47405, USA.
- [7] M.J.S. Dewar, N. Trinajstić, Chem. Commun. (1970) 646.
- [8] R.M. Minyaev, Int. J. Quantum Chem. 49 (1994) 105.
- [9] P.G. Mezey, Potential Energy Hypersurface, Studies in Physical and Theoretical Chemistry, vol. 53, Elsevier, Amsterdam, 1987.
- [10] T. Rosenfeld, M. Otolenghi, A. Meyer, Mol. Photochem. 5 (1973) 39.